IJE TRANSACTIONS C: Aspects Vol. 27, No. 6, (June 2014) 979-990

International Journal of Engineering

Journal Homepage: www.ije.ir

Analytic Approach to Free Vibration and Buckling Analysis of Functionally Graded Beams with Edge Cracks Using Four Engineering Beam Theories

K. Sherafatnia[a], G. H. Farrahi[a], S. A. Faghidian*[b]

[a]School of Mechanical Engineering, Sharif University of Technology,Tehran, Iran
[b]Department of Mechanical and Aerospace Engineering, Science and Research Branch, Islamic Azad University, Tehran, Iran

PAPER INFO

Paper history:
Received 20September2013
Received in revised form 11December2013
Accepted 12December 2013

Keywords:
Functionally Graded MaterialsSupport
Engineering Beam Theories
Open Edge Crack
Vibration Analysis
Buckling Analysis

ABSTRACT

A complete investigation on the free vibration and stability analysis of beams made of functionally graded materials (FGMs) containing open edge cracks utilizing four beam theories, Euler-Bernoulli, Rayleigh, shear and Timoshenko, is performed here. It is assumed that the material properties vary along the beam thickness exponentially and the cracked beam is modeled as two segments connected by two mass-less springs, extensional and rotational spring. Afterward the equations of motion for the free vibrations and buckling analysis are established and solved analytically for clamped-free boundary conditions. A detailed parametric study is also performed to examine the influences of the location and depth of the crack, material properties and slenderness ratio of the beam on the free vibration and buckling characteristics of cracked FGM beams for each of the four engineering beam theories.

doi:*10.5829/idosi.ije.2014.27.06c.17*

1. INTRODUCTION

Cracks as a defect in a structure, change the structural characteristics of the material, reduce the natural frequencies and affect the vibration mode shapes. Therefore, using the data of vibration analysis is a non-destructive method in order to recognize the position and depth of the edge cracks. Vibration investigations on cracked structures were performed by many researchers utilizing analytical, numerical and experimental methods. Although the early works were started by Kirmsher [1] and Thomson [2] who studied the role of crack and local discontinuity on structural characteristics, different methods were then utilized to study vibration analysis of cracked beams. These methods consist of finite element [3], Galerkin and local Ritz [4], approximate analytical approach [5], transfer matrix [6] and dynamic stiffness matrix approach [7].

In vibration analysis, cracks are usually modeled utilizing rotational and extensional spring to exhibit the reduction of the beam bending stiffness where the equivalent lumped stiffness could be calculated using fracture mechanics. In this context, Yokoyama and Chen [8] calculated the vibration characteristics of Euler-Bernoulli beam with a surface crack using lumped flexibility method and modified line-spring model. They determined the natural frequencies and the corresponding mode shapes for beams having edge cracks of different depths at different positions. In more recent studies, Zheng and Fan [9] and El Bikri et al. [10] studied free vibration analysis of beams with an edge crack while the effect of multiple cracks in a cracked beam on natural frequencies was studied by Lee [11] later.

Another aspect of present research is the stability analysis that plays an important role in many engineering structures. It is well known that cracks have undeniable effects on the equivalent stiffness and consequently the buckling load of the columns. In early works, Liebowitz et al. proposed an experimental [12] and also an analytical method [13] to determine the buckling loads of notched columns subjected to axial compressive loading.Then the stability of the cracked columns subjected to follower and vertical loads is investigated by Anifantis and Dimarogonas [14] using

*Corresponding Author Email: Faghidian@gmail.com (S. A. Faghidian)

flexibility matrix. In more recent studies, Fan and Zheng [15] investigated the stability of a cracked Timoshenko beam column using a new modified Fourier series. Also Skrinar [16] presented a new geometrical stiffness matrix for finite element modeling of a transversely cracked beam in buckling analysis according to the Euler's elastic flexural buckling theory. In addition, it should be mentioned that, FG materials are one of the latest advanced materials composed of two or more different phases. Since the materials volume percentage continuously varies from one surface to another, the material properties are varied continuously along those dimensions [17]. Considering the increasing application of FG materials in industry, many researches were performed in order to analyze their characteristics including vibration [18, 19]. Due to the enormous literature on FG materials, recent researches closely related to the current study are reviewed here. Yang and Chen [20] studied the vibration and buckling characteristics of a cracked FG beam based on the Euler-Bernoulli displacement field utilizing a rotational spring model.

Sina et al. [21] used an analytical method to investigate the free vibration of FG beams using the first order shear deformation beam theory. Then,Ke et al. [22] studied free vibrations, buckling and post-buckling of FGM Timoshenko beam containing open cracks by assuming an exponential variation of material properties in the thickness direction. Also,Simsek [23] studied free vibrations of FG beams using different higher-order shear deformation theories and derived governing equations using Hamilton's principle. Recently, Ferezqi et al. [24] presented an analytical approach based on the wave method to study the free vibrations of a FG Timoshenko beam. They investigated transverse vibration characteristics of the cracked FG Timoshenko beam with power law material property distribution. Finally analytical relations between the critical buckling load of a FG Timoshenko beam and that of the corresponding homogeneous Euler–Bernoulli beam subjected to axial compressive load have been studied by Li and Batra [25].

In the present research, an analytical method using four engineering beam theories; Euler-Bernoulli, Rayleigh, Shear and Timoshenko beam theory, are used to study the free vibration and stability of FG beams with an edge crack. A brief historical review of these engineering beam theories could be found elsewhere [26]. Afterwards the crack is modeled by two mass-less springs; extensional and rotational springs, and the equations of motion are derived using minimum total potential energy principle and solved analytically. The effects of crack position, crack depth, material properties and geometric properties of the beam on free vibration and buckling characteristics of the cracked FG beam with clamped-free boundary condition are then investigated.

2. MATERIAL PROPERTIES

The geometry of an FG beam with length L, width b_0 and thickness h is shown in Figure 1. The material property variation is assumed to be in terms of a simple power law distribution, that first introduced by Wakashima et al. [27]:

$$
\begin{aligned}
E(z) &= (E_1 - E_2)\left(\frac{2z+h}{2h}\right)^n + E_2 \\
\rho(z) &= (\rho_1 - \rho_2)\left(\frac{2z+h}{2h}\right)^n + \rho_2 \\
\upsilon(z) &= \upsilon = \text{constant}
\end{aligned}
\tag{1}
$$

where E_1 and ρ_1 are the corresponding elasticity modulus and mass density of the metal and E_2 and ρ_2 are elasticity modulus and mass density of the ceramic, respectively, and n is the non-negative variable parameter that is named volume fraction exponent.

The FG elasticity modulus and mass density of the beam could be found according to Equation (1) while considering the small variations in Poisson's coefficient, its value for an FG material is supposed to be constant along the thickness.

3. LINEAR AND ROTATIONAL SPRING MODEL

In the present analysis, the cracked FG beam is treated as two separate beams connected by two elastic springs; a rotational and an extensional spring, at the cracked section. As it is shown in Figure 2, the mass and length of springs are ignored and the crack is considered to be perpendicular to beam surface and is always open.

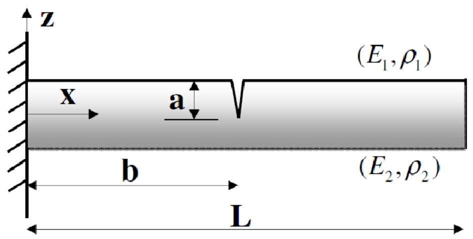

Figure 1. Cantilever FG beam containing an edge crack.

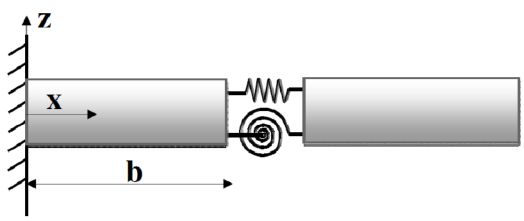

Figure 2. Model of the cracked beam section with the rotational and extensional springs.

The stiffness constant of the torsional and extensional springs used to model the edge crack is evaluated based on the relations of the fracture mechanics, considering the flexibility constants on the crack location (c_b, c_t) as follows:

$$\bar{K}_b = \frac{1}{c_b}, \quad \bar{K}_t = \frac{1}{c_t} \tag{2}$$

where $\bar{K}_b, \bar{K}_t$ are the stiffness of the beam cracked section subjected to pure bending and tension. To calculate the stiffness constants, stress intensity factors evaluated by Erdogan and Wu [28] for a cracked FG beam subjected to pure bending and tension are used:

$$K_{Ib} = \sigma_b \sqrt{\pi a} f_b\left(\frac{a}{h}, \frac{E_2}{E_1}\right); \quad K_{It} = \sigma_t \sqrt{\pi a} f_t\left(\frac{a}{h}, \frac{E_2}{E_1}\right) \tag{3}$$

Based on the formulation of the *J*-integral in plane-stress state together with considering the fact that the elastic modulus of an FG beam is function of the beam thickness (*z*), the value of the *J*-integral can be approximated by its weighted average, as [29]:

$$J = \frac{1}{h}\int_{-h/2}^{h/2} \frac{1}{E(z)} K_I^2 \, dz \tag{4}$$

Based on the fundamental relations of fracture mechanics, it is well known that the strain energy (U) for a certain value of elastic modulus ratio (E_2 / E_1) can be obtained by integration of *J* as follows:

$$\begin{aligned} U_b &= b_0 \int_0^a J_b \, da = \frac{36\pi M_b^2 \tilde{I}_b}{b_0 h^3 \tilde{D}} \\ U_t &= b_0 \int_0^a J_t \, da = \frac{\pi F_t^2 \tilde{I}_t}{b_0 h \tilde{D}} \end{aligned} \tag{5}$$

where to simplify the formulation the following constants are introduced:

$$\tilde{I}_i = \frac{1}{h^2}\int_0^a a \, f_i^2\left(\frac{a}{h}\right) da; \quad \tilde{D}^{-1} = \int_{-h/2}^{h/2} \frac{dz}{E(z)} \tag{6}$$

Also, the shape function $f_i(a/h)$ introduced in the formulation of the stress intensity factor is a famous polynomial function evaluated by Erdogan and Wu [28]. Finally to find the flexibility constants of the springs (c_b, c_t), since all relations are linear elastic, the second hypothesis of Castigiliano could be employed and the flexibility constants of the springs are found as:

$$\begin{aligned} c_b &= \frac{\partial \theta}{\partial M_b} = \frac{\partial^2 U_b}{\partial M_b^2} = \frac{72\pi \tilde{I}_b}{b_0 h^3 \tilde{D}} \\ c_t &= \frac{\partial u}{\partial F_t} = \frac{\partial^2 U_t}{\partial F_t^2} = \frac{2\pi \tilde{I}_t}{b_0 h \tilde{D}} \end{aligned} \tag{7}$$

4. FREE VIBRATION ANALYSIS

4.1. Equations of Motion

The FG beam with length *L*, thickness *h* and an edge crack in the distance *b* from the clamped end is considered as shown in Figure 1. Utilizing the principle of minimum total potential energy, the equations of motion for each of the four FG beam theories and the expression for boundary conditions are obtained. As mentioned earlier, the four beam theories are the Euler-Bernoulli, Rayleigh, shear and Timoshenko. The displacement field is defined based on shear deformation beam theory [26]:

$$\begin{aligned} u_1 &= u_0(x,t) + z\zeta(x,t) \\ u_2 &= 0 \\ u_3 &= w(x,t) \end{aligned} \tag{8}$$

where $u_0(x,t)$ and $w(x,t)$ are the axial and transverse displacement of the mid-plane of the beam and u_1, u_2 and u_3 are mid-surface displacements in the *x*, *y* and *z* directions. The rotation function of $\zeta(x,t)$ describes the difference between first order shear deformation and classic beam theory as follows:

$$\begin{aligned} \zeta(x,t) &= \varphi(x,t) \quad \text{FSDT} \\ \zeta(x,t) &= -w_{,x}(x,t) \quad \text{Classic} \end{aligned} \tag{9}$$

where $\varphi(x,t)$ denotes the rotation of the cross section and $()_{,x}$ indicates the derivative with respect to *x*. Utilizing the linear strain-displacement relation, non-zero terms of strain field could be found as:

$$\begin{aligned} \varepsilon_x &= u_{0,x} + z\zeta_{,x} \\ \gamma_{xz} &= \zeta + w_{,x} \end{aligned} \tag{10}$$

Beam problems commonly are considered as plane stress problems, so by enforcing the plane stress conditions of $\sigma_y = 0$ the only non-zero term of stress field that participates in the strain energy of the beam is:

$$\sigma_{xz} = \frac{E(z)}{2(1+\upsilon)}\left(\zeta + w_{,x}\right) \tag{11}$$

Also, governing equations of the system are derived using principle of minimum total potential energy described as [30]:

$$\int_{t_1}^{t_2} (\delta U + \delta V - \delta T)\, dt = 0 \tag{12}$$

where *U*, *T* and *V* are the potential, kinetic energy and external work of the system respectively, and t_1 and t_2 are two arbitrary times. The variation of strain energy in Equation (12) utilizing Equations (10) and (11) could be shown to be:

$$\delta U = \int_0^L \left[N(\delta u_0)_{,x} + M(\delta\zeta)_{,x} + Q\,\delta\zeta + Q(\delta w)_{,x} \right] dx \tag{13}$$

where N, M and Q are the normal resultant force, bending moment and transverse shear force, defined as:

$$N=\int_{-\frac{h}{2}}^{\frac{h}{2}}\sigma_x dz, M=\int_{-\frac{h}{2}}^{\frac{h}{2}}\sigma_x zdz, Q=\int_{-\frac{h}{2}}^{\frac{h}{2}}\sigma_{xz} dz \tag{14}$$

To rewrite the stress resultants in terms of the displacement field, the stiffness coefficients are defined as:

$$D_{ij}=\int_{-\frac{h}{2}}^{\frac{h}{2}}\tilde{E}_i(z).z^j dz;\quad \tilde{E}_1=\frac{2}{1-\upsilon};\quad \tilde{E}_2=\frac{E(z)}{1-\upsilon^2} \tag{15}$$

And the stress resultants could readily be obtained as:

$$N=D_{10}u_{0,x}+D_{11}\zeta_{,x};\ M=D_{11}u_{0,x}+D_{12}\zeta_{,x};\ Q=D_{20}(\zeta+w_{,x}) \tag{16}$$

Introducing the displacement field of Equation (10) into the standard form of kinetic energy and performing integration by parts with respect to the time, it may be shown that variation of kinetic energy has the following form [30]:

$$\int_{t_1}^{t_2}\delta T dt=-\int_{t_1}^{t_2}\int_0^L\Big[\left(I_0\ddot{u}_0+I_1\ddot{\zeta}\right)\delta u_0 +\left(I_1\ddot{u}_0+I_2\ddot{\zeta}\right)\delta\zeta+I_0\ddot{w}\delta w\Big]dxdt \tag{17}$$

In which super-script of dot shows the derivatives with respect to t and I_k is the generalized inertia moment defined as:

$$I_k=\int_{-\frac{h}{2}}^{\frac{h}{2}}\rho(z).z^k dz \tag{18}$$

Considering free vibration analysis of the beam in the absence of any external forces, the variation term related to work of the external force is zero. So the final form of the equations of motion in terms of the displacement field isobtained by substitution of Equations (13) and (17) into Equation (12) and performing some integrations by parts as follows:
For Euler-Bernoulli beam theory,

$$\begin{aligned}\delta u_0:&\quad D_{10}u_{0,xx}-D_{11}w_{,xxx}-I_0\ddot{u}_0=0\\ \delta w:&\quad D_{11}u_{0,xxx}-D_{12}w_{,xxxx}-I_0\ddot{w}=0\end{aligned} \tag{19}$$

For Rayleigh beam theory,

$$\begin{aligned}\delta u_0:&\quad D_{10}u_{0,xx}-D_{11}w_{,xxx}-I_0\ddot{u}_0+I_1\ddot{w}_{,x}=0\\ \delta w:&\quad D_{11}u_{0,xxx}-D_{12}w_{,xxxx}-I_0\ddot{w}-I_1\ddot{u}_{0,x}+I_2\ddot{w}_{,xx}=0\end{aligned} \tag{20}$$

For shear beam theory,

$$\begin{aligned}\delta u_0:&\quad D_{10}u_{0,xx}+D_{11}\varphi_{,xx}-I_0\ddot{u}_0=0\\ \delta w:&\quad D_{20}\varphi_{,x}+D_{20}w_{,xx}-I_0\ddot{w}=0\\ \delta\varphi:&\quad D_{11}u_{0,xx}-D_{20}w_{,x}-D_{20}\varphi+D_{12}\varphi_{,xx}=0\end{aligned} \tag{21}$$

For Timoshenko beam theory,

$$\begin{aligned}\delta u_0:&\quad D_{10}u_{0,xx}+D_{11}\varphi_{,xx}-I_0\ddot{u}_0-I_1\ddot{\varphi}=0\\ \delta w:&\quad D_{20}\varphi_{,x}+D_{20}w_{,xx}-I_0\ddot{w}=0\\ \delta\varphi:&\quad D_{11}u_{0,xx}-D_{20}w_{,x}-D_{20}\varphi+D_{12}\varphi_{,xx}\\ &\quad -I_1\ddot{u}_0-I_2\ddot{\varphi}=0\end{aligned} \tag{22}$$

Also, final form of the essential and natural boundary conditions is obtained as:

$$\begin{aligned}\delta u_0&=0\quad\text{or}\quad N=0\\ \delta w&=0\quad\text{or}\quad \tilde{V}=0\\ \delta\tilde{\zeta}&=0\quad\text{or}\quad M=0\end{aligned} \tag{23}$$

where $\tilde{V}$ is the effective shear force and $\tilde{\zeta}$ is the slope or rotation of the cross section of beam. The parameters of $\tilde{\zeta}$ and $\tilde{V}$ for each of four beam theories are obtained as:
For Euler-Bernoulli beam theory,

$$\tilde{\zeta}=w_{,x}\qquad \tilde{V}=M_{,x} \tag{24}$$

For Rayleigh beam theory,

$$\tilde{\zeta}=w_{,x}\qquad \tilde{V}=M_{,x}+I_2\ddot{W}_{,x}-I_1\ddot{u}_0 \tag{25}$$

For Shear and Timoshenko beam theory,

$$\tilde{\zeta}=\varphi\qquad \tilde{V}=Q \tag{26}$$

4. 2. Analytical Solution It is well known that, for harmonic vibrations, the displacement field can be expressed as:

$$\begin{aligned}u_0(x,t)&=U_0(x)e^{i\Omega t}\\ w(x,t)&=W(x)e^{i\Omega t}\\ \varphi(x,t)&=\phi(x)e^{i\Omega t}\end{aligned} \tag{27}$$

where in the above equation ($i=\sqrt{-1}$) and Ω is the natural frequency of the beam. After substituting Equation (27) into Equation (19) through Equation (22), the equations of motion for harmonic free vibrations are rewritten as:

$$\begin{aligned}&\delta U_0:\varsigma_1U_0+\varsigma_2U_0''+\varsigma_3\phi+\varsigma_4\phi''+\varsigma_5W'+\varsigma_6W'''=0\\ &\delta W:\wp_1W+\wp_2W''+\wp_3W''''+\wp_4\phi'+\wp_5U_0'\\ &\quad+\wp_6U_0'''=0\\ &\delta\phi:\chi_1\phi+\chi_2\phi''+\chi_3U_0+\chi_4U_0''+\chi_5W'=0\end{aligned} \tag{28}$$

where in Equation (28), for Euler-Bernoulli beam theory, terms of $\{\varsigma_3,\varsigma_4,\varsigma_5,\wp_2,\wp_4,\wp_5\}$ and the last relation of Equation (28), for Rayleigh beam theory, terms of $\{\varsigma_3,\varsigma_4,\wp_4\}$ and the last relation of Equation

(28), for Shear beam theory, terms of $\{\varsigma_3, \varsigma_5, \varsigma_6, \wp_3, \wp_5, \wp_6, \chi_3\}$ and finally for Timoshenko beam theory, terms of $\{\varsigma_5, \varsigma_6, \wp_3, \wp_5, \wp_6\}$ must be omitted. Then the coupled system of Equations (28) is solved and it may be shown that, axial displacement $U_0(x)$, transverse deflection $W(x)$ and rotation $\phi(x)$ are obtained as:

$$
\begin{aligned}
W(x) &= C_1 \sinh(\sqrt{\lambda_1} x) + C_2 \cosh(\sqrt{\lambda_1} x) + C_3 \sinh(\sqrt{\lambda_2} x) \\
&+ C_4 \cosh(\sqrt{\lambda_2} x) + C_5 \sinh(\sqrt{\lambda_3} x) + C_6 \cosh(\sqrt{\lambda_3} x) \\
U_0(x) &= C_2 f(\lambda_1) \sinh(\sqrt{\lambda_1} x) + C_1 f(\lambda_1) \cosh(\sqrt{\lambda_1} x) \\
&+ C_4 f(\lambda_2) \sinh(\sqrt{\lambda_2} x) + C_3 f(\lambda_2) \cosh(\sqrt{\lambda_2} x) \\
&+ C_6 f(\lambda_3) \sinh(\sqrt{\lambda_3} x) + C_5 f(\lambda_3) \cosh(\sqrt{\lambda_3} x) \\
\phi(x) &= C_2 g(\lambda_1) \sinh(\sqrt{\lambda_1} x) + C_1 g(\lambda_1) \cosh(\sqrt{\lambda_1} x) \\
&+ C_4 g(\lambda_2) \sinh(\sqrt{\lambda_2} x) + C_3 g(\lambda_2) \cosh(\sqrt{\lambda_2} x) \\
&+ C_6 g(\lambda_3) \sinh(\sqrt{\lambda_3} x) + C_5 g(\lambda_3) \cosh(\sqrt{\lambda_3} x)
\end{aligned}
\tag{29}
$$

and

$$
\vartheta_0 + \vartheta_1 \lambda + \vartheta_2 \lambda^2 + \vartheta_3 \lambda^3 = 0 \tag{30}
$$

where λ_i's are roots of Equation (30) and have different function forms of Ω for each of four beam theories. The form of $f(\lambda_i)$, $g(\lambda_i)$ and ϑ_i that are functions of stiffness coefficients, generalized inertia moments and frequency are expressed for each of four beam theories in Appendix A.

To determine the exact values of constants C_1 through C_6 appeared in Equation (29), the appropriate form of the boundary conditions must be used as described below. According to Figure 2, an FG beam with an edge crack modeled by extensional and rotational springs, is divided in two regions where the deflection $W(x)$ and slope $\phi(x)$ for each of the two regions of the beam are named using super script, i.e. for part 1 deflection and slope are denoted by $\{W^1(x)\ ,\phi^1(x)\}$, respectively. For a clamped-free boundary condition, first the clamped boundary condition at x=0 is applied to the first part of the cracked beam, then the free-end boundary condition at x=L is applied to the second part of the cracked beam. These boundary conditions are extracted from the general form of the boundary conditions described in Equation (23) as:

$$
\begin{aligned}
&U_0^1 = 0,\ W^1 = 0,\ \tilde{\zeta}^1 = 0 \quad \text{Clamped at } x = 0 \\
&N^2 = 0,\ \tilde{V}^2 = 0,\ M^2 = 0 \quad \text{Free-end at } x = L
\end{aligned}
\tag{31}
$$

The other boundary conditions at x=b near the crack position, based on spring model are described as:

at $x = b$:

$$
\begin{aligned}
&K_t(U_0^2 - U_0^1) = N^1, \qquad W^1 = W^2 \\
&K_b(\tilde{\zeta}^2 - \tilde{\zeta}^1) = M^1, \qquad N^1 = N^2 \\
&\tilde{V}^1 = \tilde{V}^2, \qquad M^1 = M^2
\end{aligned}
\tag{32}
$$

Replacing of Equation (16) and Equation (24) through Equation (26) and Equation (29) into Equation (31) and Equation (32) will result in a matrix of equations of:

$$
[B(\lambda)]\{C\} = 0 \tag{33}
$$

Using the familiar concepts of linear algebra, it may be shown that this set of equations has a non-trivial solution when its determinant is equal to zero:

$$
\det[B(\lambda)] = |B(\lambda)| = 0 \tag{34}
$$

Finally natural frequencies and the different mode shapes of the cracked FG beam are obtained bysolving Equation (34).

5. BUCKLING ANALYSIS

5. 1. Equilibrium Equations To analyze the stability of the FG beam with an edge crack, an axial compressive load is applied to the beam. For bulking analysis, non-zero terms of strain field can be expressed utilizing Von-Karman theory as [31]:

$$
\begin{aligned}
\varepsilon_x &= u_{1,x} + \frac{1}{2} u_{3,x}^2 \\
\gamma_{xz} &= u_{1,z} + u_{3,x}
\end{aligned}
\tag{35}
$$

Substituting displacement field of Equation (8) into Equation (35) and utilizing the results in stress-strain relations of plane stress conditions, the only non-zero term of stress field that participates in the strain energy of the beam is σ_{xz} with the same relation of Equation (11). Also the equilibrium equations are obtained using the principle of minimum total potential energy. It should be noted that, since stability analysis is a static analysis, the term of kinetic energy is omitted from principle of minimum total potential energy of Equation (12), while the effect of external compressive load on the total virtual work is considered in the potential energy [32]. The virtual work of the external compressive load P (per unit width) is given by:

$$
\begin{aligned}
\delta U_P &= \int_0^L \int_A -\left(\frac{P}{A}\right) \varepsilon_{xx}\, dA\, dx \\
&= \left(\frac{-P}{h}\right) \int_0^L \int_{-\frac{h}{2}}^{\frac{h}{2}} \left(\delta u_{0,x} + z\delta\zeta_{,x} + w_{,x}\delta w_{,x}\right) dz dx
\end{aligned}
\tag{36}
$$

And the variation of strain energy may be shown to be:

$$\delta U_s = \int_{-\frac{h}{2}}^{\frac{h}{2}}\int_0^L \Big[N\,(\delta u_0)_{,x} + M\,(\delta\zeta)_{,x} + N w_{,x}\,(\delta w)_{,x} + Q\,\delta\zeta + Q\,(\delta w)_{,x} \Big] dx dz \qquad (37)$$

where in Equation (37), the stress resultants N, M and Q have the same definition as Equation (14).

The equilibrium equations may be obtained using principle of minimum total potential energy while performing integration by parts and omitting the kinetic energy and work of external force in buckling analysis. For each of the four beam theories, the equilibrium equations may be shown to be:

For Euler-Bernoulli and Rayleigh beam theories,

$$\begin{aligned} \delta u_0 &: \quad D_{10}u_{0,xx} - D_{11}w_{,xxx} = 0 \\ \delta w &: \quad D_{11}u_{0,xxx} - D_{12}w_{,xxxx} - Pw_{,xx} = 0 \end{aligned} \qquad (38)$$

For Timoshenko and Shear beam theories,

$$\begin{aligned} \delta u_0 &: \quad D_{10}u_{0,xx} + D_{11}\varphi_{,xx} = 0 \\ \delta w &: \quad D_{20}\varphi_{,x} + D_{20}w_{,xx} - Pw_{,xx} = 0 \\ \delta\varphi &: \quad D_{11}u_{0,xx} - D_{20}w_{,x} - D_{20}\varphi + D_{12}\varphi_{,xx} = 0 \end{aligned} \qquad (39)$$

The final form of the geometry (kinematic) boundary conditions and the force (static) boundary conditions are also obtained as:

$$\begin{aligned} \delta u_0 &= 0 \quad \text{or} \quad \tilde{N} = -P \\ \delta w &= 0 \quad \text{or} \quad \tilde{V} = 0 \\ \delta\zeta &= 0 \quad \text{or} \quad M = 0 \end{aligned} \qquad (40)$$

where the axial resultants $\{\tilde{N}, \tilde{V}\}$ are defined for Euler-Bernoulli and Rayleigh beam theories as,

$$\tilde{N} = N - P, \qquad \tilde{V} = M_{,x} - Pw_{,x} \qquad (41)$$

and for Timoshenko and Shear beam theories as,

$$\tilde{N} = N - P, \qquad \tilde{V} = Q - Pw_{,x} \qquad (42)$$

5. 2. Analytical Solution

The coupled system of equations (Equations (38) and (39)) are then solved separately and it may be shown that, the axial displacement $u_0(x)$, transverse deflection $w(x)$ and rotation $\phi(x)$ are obtained as:

For Euler-Bernoulli and Rayleigh beam theories,

$$\begin{aligned} w(x) &= \frac{\tilde{C}_1 \sinh(\sqrt{\tilde{\lambda}}x) + \tilde{C}_2 \cosh(\sqrt{\tilde{\lambda}}x)}{\tilde{\lambda}} + \tilde{C}_3 x + \tilde{C}_4 \\ u_0(x) &= \tilde{\varsigma} w_{,x} + \tilde{C}_5 x + \tilde{C}_6 \end{aligned} \qquad (43)$$

where $\tilde{\lambda}$ and $\tilde{\varsigma}$ are expressed as,

$$\tilde{\lambda} = \frac{PD_{10}}{D_{11}^2 - D_{10}D_{12}}, \quad \tilde{\varsigma} = \frac{D_{11}}{D_{10}} \qquad (44)$$

For Timoshenko and Shear beam theories,

$$\begin{aligned} w(x) &= \frac{\tilde{C}_1 \sinh(\sqrt{\tilde{\lambda}}x) + \tilde{C}_2 \cosh(\sqrt{\tilde{\lambda}}x)}{\tilde{\lambda}\sqrt{\tilde{\lambda}}} + \tilde{C}_3 x + \tilde{C}_4 \\ \varphi(x) &= -w_{,x} + \frac{\tilde{\wp}}{\tilde{\lambda}} w_{,xxx} \\ u_0(x) &= \tilde{\chi} w_{,x} + \tilde{C}_5 x + \tilde{C}_6 \end{aligned} \qquad (45)$$

where $\tilde{\lambda}$, $\tilde{\wp}$ and $\tilde{\chi}$ are expressed as,

$$\begin{aligned} \tilde{\lambda} &= \frac{PD_{10}D_{20}}{(D_{11}^2 - D_{10}D_{12})(D_{20} - P)} \\ \tilde{\wp} &= \frac{P}{D_{20}} \\ \tilde{\chi} &= \frac{(D_{20} - P)D_{11}}{D_{10}D_{20}} \end{aligned} \qquad (46)$$

The unknown coefficients, $\tilde{C}_1$ to $\tilde{C}_6$ appeared in Equations (43) and (45), could be determined utilizing the similar procedure described in previous section using appropriate forms of the boundary conditions. Again the cracked FG beam is divided by an edge crack into two regions. Boundary conditions for each part of the cantilever cracked beam at x=0, x=L and x=b are similar to the Equation (31) and Equation (32), respectively. For the stability analysis, similar to the vibration analysis, critical buckling load and buckling mode shapes are obtained solving Equation (33) and Equation (34).

6. NUMERICAL RESULTS AND DISCUSSION

To compare the results of the current study with other researches, the dimensionless frequency and dimensionless critical buckling load are defined as fundamental frequency ratio$\omega_1/\omega_{10}$and critical buckling load ratio$P_{cr}/\ P_{cr0}$whereω_1, ω_{10}, , $P_{cr}$and$P_{cr0}$are representations of first natural frequency and critical buckling load of cracked and flawless (un-cracked) beam, respectively.

In Table 1 dimensionless first natural frequencies are calculated for a homogeneous cracked beam with clamped free boundary condition and the results are compared to the experimental data obtained by Wendtland [33]. The geometric and material properties of the sample beam are supposed to be the same as given by Wendtland [33] that are reported as, length 200 mm, thickness 7.8 mm, Young modulus 206 GPa, density 7800 Kg/m^3, Poisson ratio 0.29 with different crack depths and locations. The predicted frequencies are in excellent agreement with the experimental results. Again to examine the accuracy of the present analytical results, dimensionless first natural frequencies and critical buckling loads are compared to Yang and Chen [20] and tabulated in Table 2. To this end, a functionally graded cantilever beam with an edge crack is considered with material and geometrical characteristics of L/h=10, a/h=0.2, E_1=70GPa, n=1.9, $\nu = 0.33$ and position of the crack b/L=0.4, similar specifications to Yang and Chen [20]. Also, to match the exponential material behavior of Yang and Chen [20] with power law material behavior of current study, Equation (1), the value of volume fraction exponent n is considered to be 1.9. As it may be seen from Table 2, the results are in good agreement with Yang and Chen [20] and little differences observed in the results is due to different crack models used.

Natural frequencies, buckling critical loads and vibration and buckling mode shapes of the four beam theories; Euler-Bernoulli, Rayleigh, shear and Timoshenko are then compared together and presented in the followings. The material properties and geometry data used here in free vibration and stability analysis of the cracked FG beam are selected as elastic modulus of metal, E_1=70GPa, Poisson's ratio, $\nu = 0.3$, mass density of metal, $\rho_1 = 2700\,Kg/m^3$, elastic modulus (and mass density) ratio, $(E_2/E_1), (\rho_2/\rho_1) = 0.2$ with crack depth ratio of a/h=0.3 and beam slenderness ratio of L/h=10 with crack located at b/L=0.4. The metal phase material properties are selected similar to Yang and Chen [20].

The dimensionless k-th natural-frequency ratio (ω_k/ω_{k0}) and dimensionless buckling load ratio (p_{cr}/p_{cr0}) are respectively shown in Figures 3 and 5 versus the crack location. In should be noted that ω_k represents the k-th natural frequency of the cracked FG beam while ω_{k0} denotes the k-th natural frequency of the beam with no crack. Similarly, the buckling load of the functionally graded beam with and without crack is represented by P_{cr} and P_{cr0}, respectively. Also the first three transverse vibration mode shapes are exhibited in Figure 4.

It is inferred from Figure 3 that as the crack location approaches the clamed end, the effect of the crack on the reduction of the frequency ratio is more obvious. Moreover, when the crack location is close to the free-end, the cracked beam natural frequencies approaches the natural frequencies of the flawless (un-cracked) beam. Again from Figure 3 it can be seen that the order of the natural frequency ratio values of four theories from maximum to minimum is Shear, Timoshenko, Euler-Bernoulli and Rayleigh. Also it is interesting to note that the second and the third frequency ratios have two and three maximum value with different crack location, while the location of edge crack where the second and the third frequencies achieve maximum value is different for four models. Furthermore, it is important to note that, since the ratio of the first natural frequency increases continually as the crack location approaches the free-end, it can be concluded that the first natural frequency will be more useful in order to detect the crack location experimentally.

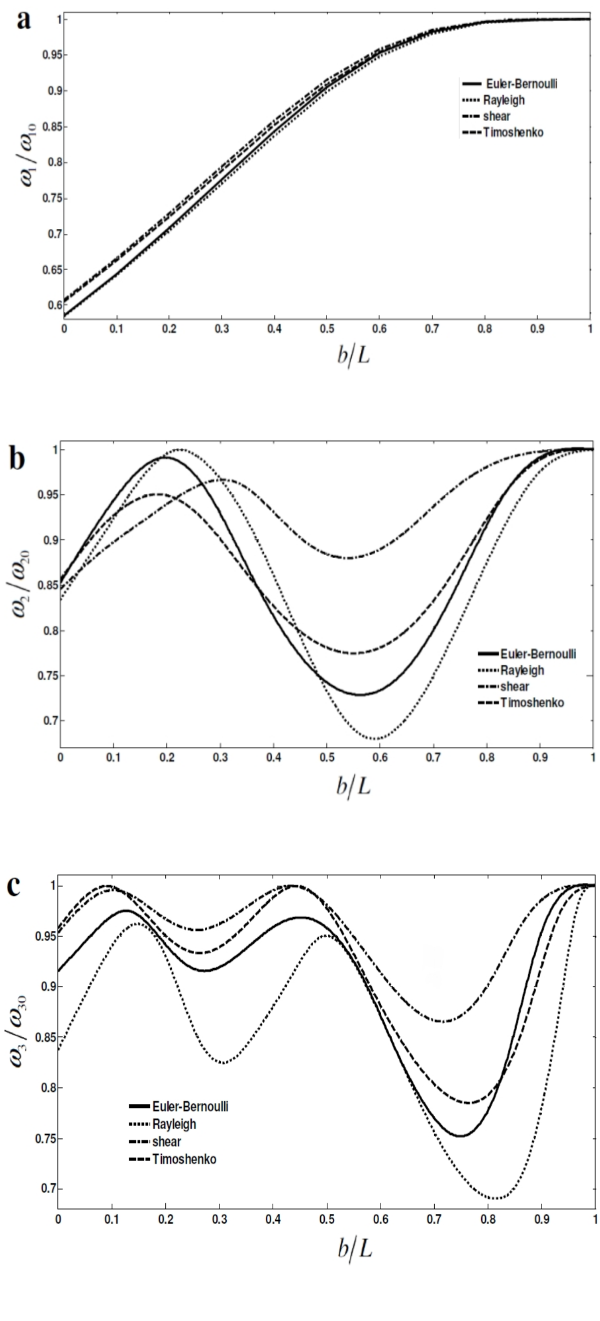

Figure 3. The first three frequency ratio of cantilever FG beams for four beam theories at varying locations of crack: a) first frequency ratio, b) second frequency ratio and c) third frequency ratio

Figure 4 shows the first three transverse vibration mode shapes of the cracked FG beam while the mode shapes are normalized with respect to their maximum values. It is interesting to note that as expected and seen from Figure 4, the first vibration mode shapes of all beam theories are very close together, while the second and the third ones are different meaningfully.The effect of the crack location on the buckling load ratio is exhibited in Figure 5.

It is observed that the crack location has a significant effect on the buckling load of the FG beam. In addition, it can be seen that the buckling load decreases as the crack location approaches the clamped-end of the beam. Also when the crack is located close to the free-end, the difference between the buckling loads of the cracked beam and those of the beam without crack diminishes. Figure 5 shows that buckling load ratio of Timoshenko beam is higher than that of Euler-Bernoulli beam, which was observed in results of Zheng and Fan [9] for a column with an open crack with variable location.

The ratios of the first natural frequencies of a cracked FG beam (ω_1/ω_{10}) are given in Table 3 for different Young's modulus ratios and for n=0.2,5 . The Young's modulus ratio (E_2/E_1) is defined as the ratio of the elastic modulus of the bottom surface, the surface without crack, to the elastic modulus of the top surface, the surface with crack. As it is expected, the values of fundamental (first) frequency ratio of Timoshenko and Shear theories are close to each other while results of Euler and Rayleigh theories are close together too. Also it is clear from Table 3 that the effect of the crack on the reduction of the natural frequencies of the FG beam is more obvious when the modulus ratio (E_2/E_1) is low.

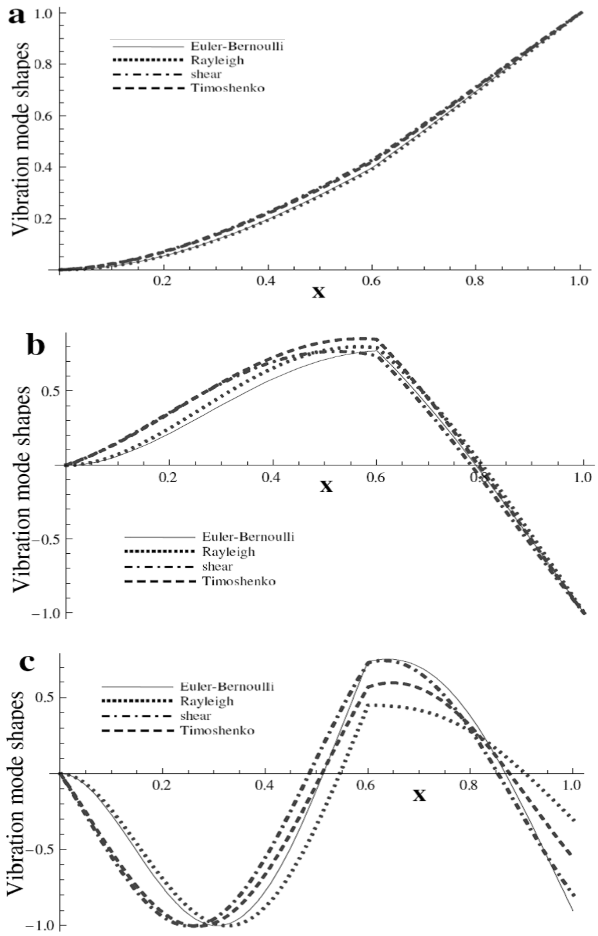

Figure 4. The first three transverse vibration mode shapes of a cantilever FG beam with b/L=0.6, a) first, b) second and c) third transverse vibration mode shape.

TABLE 1. Comparison of fundamental frequency ratio (ω_1/ω_{10}) of a cracked beam with experimental results of Wendtland [33].

	***b/L*=0.025**			***b/L*=0.2**			***b/L*=0.4**		
a/h	0.13	0.26	0.4	0.13	0.26	0.4	0.13	0.26	0.4
Present study (Timoshenko model)	0.986	0.949	0.878	0.992	0.970	0.926	0.997	0.988	0.968
Wendtland [33]	0.987	0.957	0.891	0.991	0.973	0.931	0.997	0.989	0.970

TABLE 2. Comparison of fundamental frequency and critical buckling load ratio of a cracked FG beam with results of Yang and Chen [20]

	Fundamental frequency ratio				**Buckling load ratio**			
L/h	10		20		10		20	
E_2/E_1	0.2	5	0.2	5	0.2	5	0.2	5
Present study (EB beam)	0.951	0.993	0.974	0.997	0.870	0.981	0.931	0.990
Yang and Chen [20]	0.985	0.998	0.992	0.999	0.956	0.997	0.977	0.998

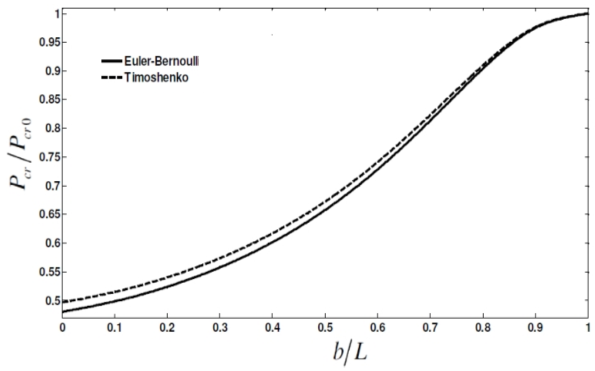

Figure 5. The critical buckling load ratio of cantilever FG beams for two beam theories versus varying locations of the crack.

TABLE 3. Fundamental frequency ratio of cantilever FG beams with an edge crack for various elastic modulus ratios

E_2/E_1	*n*	Euler-Bernoulli	Rayleigh	Shear	Timoshenko
0.2	0.2	0.9130	0.9129	0.9139	0.9137
10		0.9862	0.9861	0.9863	0.9863
0.2	5	0.8877	0.8873	0.8889	0.8885
10		0.9879	0.9879	0.9880	0.9880

TABLE 4. The fundamental frequency ratio of cantileverFG beams with an edge crack for various slenderness ratios

L/h	*n*	Euler-Bernoulli	Rayleigh	Shear	Timoshenko
5	0.2	0.8448	0.8436	0.8501	0.8489
20		0.9537	0.9537	0.9538	0.9537
5	5	0.8062	0.8035	0.8129	0.8102
20		**0.9390**	**0.9390**	**0.9392**	0.9391

TABLE 5. The fundamental frequency ratio of cantilever FG beams with an edge crack for various crack depth ratios

a/h	Euler-Bernoulli	Rayleigh	Shear	Timoshenko
0.2	0.9510	0.9508	0.9515	0.9513
0.4	0.8382	0.8377	0.8395	0.8390

TABLE 6. The critical buckling load ratio of cantilever FG beams with an edge crack for various elastic modulus ratios

E_2/E_1	*n*	Euler-Bernoulli	Timoshenko
0.2	0.2	0.7607	0.7618
10		0.9583	0.9585
0.2	5	0.7009	0.7022
10		0.9635	0.9637

TABLE 7. The critical buckling load ratio of cantilever FG beams with an edge crack for various slenderness ratios

L/h	*n*	Euler-Bernoulli	Timoshenko
5	0.2	0.6093	0.6146
20		0.8657	0.8659
5	5	0.5343	0.5403
20		0.8265	0.8267

In Table 4, the variation of the fundamental frequency ratios with length to thickness ratio (*L/h*) are shown for two values of power law exponent, *n*. The results in Table 4 show that, when the beam becomes more slender, the first natural frequency of the beam becomes closer to the natural frequency of the flawless (un-cracked) beam.It is also clear that for high values of length to thickness ratio, difference among all four beam theories becomes negligible.It is observed from Table 5 that by increasing the depth of crack, natural frequency ratios decreases exhibiting that natural frequency of cracked beam differ more from a flawless (un-cracked) beam, as it was expected.

Tables 6 and Table 7 tabulate the critical buckling load ratio of a cracked FG beam with different Young's modulus ratios and slender ratios, respectively. As it is shown in analytical solution of the stability analysis, the results of Euler-Bernoulli and Rayleigh models are identical and also the buckling load ratios and mode shapes of the shear model are identical to those of the Timoshenko model.

As it is seen from Table 6, when the modulus ratio (E_2/E_1) becomes higher, the buckling loads of the cracked beam approaches those of the beam without crack. Moreover, it is deduced that the reduction of the elastic modulus of the cracked surface has an increasing effect on the buckling load.Also, results of Table 7 indicate that as the ratio of the beam length to the beam thickness (*L/h*) increases, the effect of the crack on the reduction of the buckling load diminishes and for the high values of (*L/h*), the beams with and without cracks and also Timoshenko and Euler-Bernoulli modelshave approximately the same responses. By the way, it can be deduced from Tables 6 and Table 7 that the buckling ratios of Timoshenko model has more value rather than those of Euler model.

7. CONCLUSIONS

In the present research, an analytical method is presented to investigate the free vibration and buckling analysis of FG beams with an open edge crack. A comprehensive study is done here to examine the effects of parameters such as location of cracks, depth of cracks, material properties of FG and slenderness ratio on the natural frequencies, critical buckling load and their mode shapes for each of the four engineering beam theories; Euler-Bernoulli, Rayleigh, shear and Timoshenko.

It is generally observed that the natural frequency ratios obtained using shear model is greater than those of others considering effects of different parameters. After shear model, Timoshenko, Euler-Bernoulli and Rayleigh model are next in rank, respectively. It can be also deduced that considering the shear deformation in cracked beam model leads to increase the natural frequency ratio while adding the rotary inertia in model decreases the frequency ratio. However, it seems that the results of Timoshenko beam theory are in better agreement with the experimental results. Also, results confirm that the effect of shear deformation is more dominant than the effect of rotary inertia on frequency ratio. By the way, the effect of shear on buckling ratios of cracked FG column in stability analysis is similar to vibration analysis.

In addition, the results confirm that existence of cracks in the beam reduces natural frequencies and critical buckling loads and causes significant change in vibration and buckling mode shapes. The results also show that cracked FG beams with lower slenderness ratio and beams with the edge crack closer to the support and beams with lower elasticity modulus ratio in the surface containing the edge crack, are more affected by the crack and their natural frequencies and critical buckling loads is reduced further.

8. REFERENCES

1. Kirmser, P.G., "The effects of discontinuities on the natural frequency of beams, The College, (1945).
2. Thomson, W., "Vibration of slender bars with discontinuities in stiffness", ***Journal of Applied Mechanics-Transactions of the Asme***, Vol. 16, No. 2, (1949), 203-208.
3. Krawczuk, M. and Ostachowicz, W., "Modelling and vibration analysis of a cantilever composite beam with a transverse open crack", ***Journal of Sound and Vibration***, Vol. 183, No. 1, (1995), 69-89.
4. Shen, M.-H. and Pierre, C., "Free vibrations of beams with a single-edge crack", ***Journal of Sound and Vibration***, Vol. 170, No. 2, (1994), 237-259.
5. Narkis, Y., "Identification of crack location in vibrating simply supported beams", ***Journal of Sound and Vibration***, Vol. 172, No. 4, (1994), 549-558.
6. Tsai, T. and Wang, Y., "Vibration analysis and diagnosis of a cracked shaft", ***Journal of Sound and Vibration***, Vol. 192, No. 3, (1996), 607-620.
7. Khiem, N. and Lien, T., "The dynamic stiffness matrix method in forced vibration analysis of multiple-cracked beam", ***Journal of Sound and Vibration***, Vol. 254, No. 3, (2002), 541-555.
8. Yokoyama, T. and Chen, M.-C., "Vibration analysis of edge-cracked beams using a line-spring model", ***Engineering Fracture Mechanics***, Vol. 59, No. 3, (1998), 403-409.
9. Zheng, D. and Fan, S., "Natural frequency changes of a cracked timoshenko beam by modified fourier series", ***Journal of Sound and Vibration***, Vol. 246, No. 2, (2001), 297-317.
10. El Bikri, K., Benamar, R. and Bennouna, M., "Geometrically non-linear free vibrations of clamped–clamped beams with an edge crack", ***Computers & Structures***, Vol. 84, No. 7, (2006), 485-502.
11. Lee, J., "Identification of multiple cracks in a beam using natural frequencies", ***Journal of Sound and Vibration***, Vol. 320, No. 3, (2009), 482-490.
12. Liebowitz, H., Vanderveldt, H. and Harris, D., "Carrying capacity of notched columns", ***International Journal of Solids and Structures***, Vol. 3, No. 4, (1967), 489-500.
13. Liebowitz, H. and Claus Jr, W., "Failure of notched columns", ***Engineering Fracture Mechanics***, Vol. 1, No. 2, (1968), 379-383.
14. Anifantis, N. and Dimarogonas, A., "Stability of columns with a single crack subjected to follower and vertical loads", ***International Journal of Solids and Structures***, Vol. 19, No. 4, (1983), 281-291.
15. Fan, S.C. and Zheng, D., "Stability of a cracked timoshenko beam column by modified fourier series", ***Journal of Sound and Vibration***, Vol. 264, No. 2, (2003), 475-484.
16. Skrinar, M., "Improved beam finite element for the stability analysis of slender transversely cracked beam-columns", ***Computational Materials Science***, Vol. 45, No. 3, (2009), 663-668.
17. Kargarnovin, M., Faghidian, S. and Arghavani, J., "Limit analysis of fgm circular plates subjected to arbitrary rotational symmetric loads", ***International Journal of Mechanical Systems Science & Engineering***, Vol., No., (2007).
18. Vel, S.S. and Batra, R., "Three-dimensional exact solution for the vibration of functionally graded rectangular plates", ***Journal of Sound and Vibration***, Vol. 272, No. 3, (2004), 703-730.
19. Xiang, H. and Yang, J., "Free and forced vibration of a laminated fgm timoshenko beam of variable thickness under heat conduction", ***Composites Part B: Engineering***, Vol. 39, No. 2, (2008), 292-303.
20. Yang, J. and Chen, Y., "Free vibration and buckling analyses of functionally graded beams with edge cracks", ***Composite Structures***, Vol. 83, No. 1, (2008), 48-60.
21. Sina, S., Navazi, H. and Haddadpour, H., "An analytical method for free vibration analysis of functionally graded beams", ***Materials & Design***, Vol. 30, No. 3, (2009), 741-747.
22. Ke, L.-L., Yang, J., Kitipornchai, S. and Xiang, Y., "Flexural vibration and elastic buckling of a cracked timoshenko beam made of functionally graded materials", ***Mechanics of Advanced Materials and Structures***, Vol. 16, No. 6, (2009), 488-502.
23. Şimşek, M., "Fundamental frequency analysis of functionally graded beams by using different higher-order beam theories", ***Nuclear Engineering and Design***, Vol. 240, No. 4, (2010), 697-705.
24. Ferezqi, H.Z., Tahani, M. and Toussi, H.E., "Analytical approach to free vibrations of cracked timoshenko beams made of functionally graded materials", ***Mechanics of Advanced Materials and Structures***, Vol. 17, No. 5, (2010), 353-365.
25. Li, S.-R. and Batra, R.C., "Relations between buckling loads of functionally graded timoshenko and homogeneous euler–bernoulli beams", ***Composite Structures***, Vol. 95, No., (2013), 5-9.
26. Han, S.M., Benaroya, H. and Wei, T., "Dynamics of transversely vibrating beams using four engineering theories", ***Journal of Sound and Vibration***, Vol. 225, No. 5, (1999), 935-988.
27. Wakashima, K., Hirano, T. and Niino, M., "Functionally gradient materials (fgm) architecture: A new type of ceramic-metal assemblage designed for hot structural components", in Proc. of the ESA Symp. on Space Applications of Advanced Structural Materials ESTEC-ESA, Proc. of the ESA Symp. on Space Applications of Advanced Structural Materials (ESA SP-303), (1990), 97-102.

28. Erdogan, F. and Wu, B., "The surface crack problem for a plate with functionally graded properties", ***Journal of Applied Mechanics***, Vol. 64, No. 3, (1997), 449-456.
29. Stephens, R.I. and Fuchs, H.O., "Metal fatigue in engineering, Wiley New York, (2001).
30. Cassel, K.W., "Variational methods with applications in science and engineering, Cambridge University Press, (2013).
31. Fung, Y.-C., "Foundations of solid mechanics", (1965).
32. Timoshenko, S.P., Gere, J.M. and Prager, W., "Theory of elastic stability", ***Journal of Applied Mechanics***, Vol. 29, (1962), 220.
33. Wendtland, D., "Aenderung der biegeeigenfrequenzen einer idealisierten schaufel durch risse", University of Karlsruhe, PhD thesis, (1972),

APPENDIX

Forms of the functions $f(\lambda_i)$, $g(\lambda_i)$ and ϑ_i in four engineering beam theories, appeared in Equation (29) and Equation (30), may be shown to be, for Rayleigh theory:

$$
\begin{aligned}
f(\lambda_i) &= \frac{1}{\sqrt{\lambda_i}\,\Omega^2(D_{11}I_0 - D_{10}I_1)}\Big(D_{10}I_0\Omega^2 \\
&\quad + \lambda_i\Omega^2(D_{11}I_1 - D_{10}I_2) + \lambda_i^{\,2}(D_{11}{}^2 - D_{10}D_{12})\Big) \\
\vartheta_0 &= I_0{}^2\Omega^4 \\
\vartheta_1 &= \Omega^2(D_{10}I_0 + I_1{}^2\Omega^2 - I_0I_2\Omega^2) \\
\vartheta_2 &= \Omega^2(-D_{12}I_0 + 2D_{11}I_1 - D_{10}I_2) \\
\vartheta_3 &= D_{11}{}^2 - D_{10}D_{12}
\end{aligned}
\tag{A.1}
$$

Functions $f(\lambda_i)$, $g(\lambda_i)$ and ϑ_i for Euler-Bernoulli theory are the same as relations (A.1) except that I_1 and I_2 are equal to zero .

For Timoshenko theory:

$$
\begin{aligned}
f(\lambda_i) &= \frac{1}{D_{20}(D_{11}I_0 - D_{10}I_1)\Omega^2\sqrt{\lambda_i}}\Big((I_0\Omega^2 + D_{20}\lambda_i) \\
&\quad \times(\lambda_i(D_{11}{}^2 - D_{12}D_{10}) + \Omega^2(D_{11}I_1 - D_{10}I_2) \\
&\quad + D_{10}D_{20}) + D_{10}D_{20}{}^2\lambda_i\Big) \\
g(\lambda_i) &= -\frac{I_0\Omega^2 + D_{20}\lambda_i}{D_{20}\sqrt{\lambda_i}} \\
\vartheta_0 &= I_0\Omega^4(\Omega^2(I_0I_2 - I_1{}^2) - D_{20}I_0) \\
\vartheta_1 &= \Omega^2(-D_{10}D_{20}I_0 + \Omega^2(I_0(D_{12}I_0 + D_{10}I_2 - 2D_{11}I_1) \\
&\quad + D_{20}(I_0I_2 - I_1{}^2))) \\
\vartheta_2 &= \Omega^2(D_{20}(D_{10}I_2 + D_{12}I_0 - 2D_{11}I_1) \\
&\quad + I_0(D_{12}D_{10} - D_{11}{}^2)) \\
\vartheta_3 &= D_{20}(D_{12}D_{10} - D_{11}{}^2)
\end{aligned}
\tag{A.2}
$$

Functions $f(\lambda_i)$, $g(\lambda_i)$ and ϑ_i for Shear theory are the same as relations (A.2), except that I_1 and I_2 are equal to zero.

Analytic Approach to Free Vibration and Buckling Analysis of Functionally Graded Beams with Edge Cracks Using Four Engineering Beam Theories

K. Sherafatnia [a], G. H. Farrahi [a], S. A. Faghidian[b]

[a]School of Mechanical Engineering, Sharif University of Technology, Tehran, Iran
[b]Department of Mechanical and Aerospace Engineering, Science and Research Branch, Islamic Azad University, Tehran, Iran

PAPER INFO

Paper history:
Received 20 September 2013
Received in revised form 11December 2013
Accepted 12December 2013

Keywords:
Functionally graded materials Support
Engineering beam theories
Open edge crack
Vibration analysis
Buckling analysis

چکیده

در پژوهش حاضر ارتعاشات آزاد و آنالیز پایداری تیرهای دارای ترک لبه ای و ساخته شده از مواد FG با استفاده از چهار تئوری مهندسی تیر اویلر-برنولی، رایلی، تئوری برشی و تیموشنکو بررسی شده اند. رفتار مادی تیر در راستای ضخامت آن بصورت نمایی فرض شده و ترک لبه ای نیز به کمک دو فنر بدون جرم کششی و پیچشی مدلسازی شده است. سپس معادلات حاکم بر ارتعاشات آزاد و تحلیل کمانش تیر به کمک روش انرژی بدست آمده و به صورت تحلیلی برای شرایط مرزی تیر یکسر درگیر حل شده اند. هم چنین تاثیرات مکان و عمق ترک، خواص مادی و نسبت رعنایی تیر بر فرکانس طبیعی و شکل مود های ارتعاشات آزاد و مشخصه های کمانشی تیر نیز با استفاده از هر یک از چهار تئوری مهندسی تیر کاملا بررسی شده اند.

doi:*10.5829/idosi.ije.2014.27.06c.17*